A density functional theory (DFT) calculation and vibrational analysis of smeathxanthone A

Axel Lontsi Tiwa[1, 2*] and Alembert Tiabou Tchinda[1]
[1]Institute of Medical Research and Medicinal Plants Studies (IMPM), P.O. Box 6163, Yaoundé, Cameroon
[2]Department of Organic Chemistry, University of Yaoundé I, P.O Box 812, Yaoundé, Cameroon
adonmage@gmail.com

Abstract

Natural products are now a source of many drugs for the pharmaceutical industry. For this reason, there has been an increased focus on phytochemistry over the world, which has led to the isolation of many natural substances. Herein we report molecular structure and vibrational analysis of a secondary metabolite, smeathxanthone A. high level computational theory employing M06 coupled with 6-311G simple basis set were used. Infrared data have been computed, scaled with a standard value and compared with the experimental one. We also report Fukui functions and electrostatic potential surfaces maps to study chemically reactive moieties and qualitative structure-activity relationships (QSAR). HOMO-LUMO energy gap and optimized geometry parameters have been also computed.

Introduction

Didenzoγ-pyrone also called xanthones is a secondary metabolite found in stem barks, leaves, roots of some tropical higher plants, lichens and even endophytes[1]. Since decades, many xanthones have been isolated from wildlife[2]. They are generally actives compounds, possessing many pharmacological properties, including anti-oxidant, anticancer, actives against many microbial species and can often act as hypotensive[1,3]. Recently Komguem et al. have isolated 2-(3,7-Dimethyl-2,6-octadienyl)-1,3,5,8-tetrahydroxyxanthone (smeathxanthone A) from *Garcinia smeathmannii*[4]. The structure is depicted in fig.1.Infrared spectroscopy in xanthonoids structure elucidation is mainly used to detect vibrational modes of different moieties such as phenyl groups, alkene fragments and many carbonyl groups[5], while ^{1}H and ^{13}C NMR spectroscopies give more accurate data useful to locate atoms position. To the best of our knowledge, few works have been done using computational chemistry to study molecular structures and electrostatic potential of compounds belonging to the dibenzoγ-pyronefamily[6-8]. Here in we report some structural parameters, molecular structure analysis and electronic properties of smeathxanthone A using DFT methods.
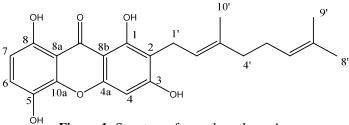

Figure-1: Structure of smeathxanthone A.

Methodology

The optimized structure has been performed using M06/6-311G DFT with water as solvent[9]. After having established the necessity to exclude any symmetry constraint we have computed the data using the Jaguar program[10]. Electrostatic potential and molecular orbitals simulations were calculated using B3LYP /6-311G. Becke, three-parameter and Lee-Yang-Parr exchange theory is a now popular method in computational chemistry which was firstly developed as an enhancement of the *ab initio* Hartree-Fock level theory. B3LYP DFT is very powerful to predict physicochemical properties, spectroscopic data, transition states and zero-point energies among others[11-12]. Fukui functions have been obtained at B3LYP/LACVP *+ level of theory. Three dimensional illustrations were performed with] Maestro 2016-1graphical interface.

Results and discussion

Geometry optimization: The crystal structure of smeathxanthone A has been determined and is illustrated in Figure-2[13]. Since the optimization has been done in water phase to mimic biological conditions, the optimized structure shown in Figure-3 illustrates some difference with the crystal one. The very visible one is the orientation of hydroxyl group at position 4 which is oriented towards the geranylsubstituent, whereas it is oriented towards the hydrogen at position 5 for the crystal structure. Crystal structure possesses bond angles C3'C2'C1' [127.4° (2)] and C7'C6'C5' [128.8° (2)] in the geranyl substituent which are in good agreement with compute angles 127.7° and 126.6° respectively]. Table-1 presents some calculated and experimental data of smeathxanthone A.
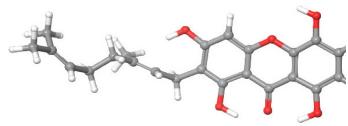
Figure-2: Optimized structure of smeathxanthone A.

Table-1: Selected molecular structure parameters.

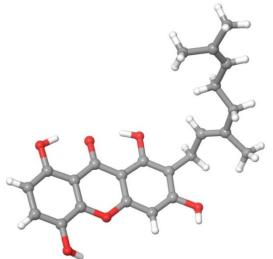| Parameters (A°)	Experimental	Calculated
C8-C8A	1.408(3)	1.41
C1-C9A	1.421(3)	1.45
C7-C8	1.374(3)	1.39
C7-C6	1.384(3)	1.39
C6-C5	1.377(3)	1.39
C1-C2	1.383(3)	1.40
C2-C3	1.405(3)	1.41
C3-C4	1.385(3)	1.39
C4-C4A	1.368(3)	1.38

Figure-3: Crystal structure of smeathxanthone A.

Vibrational analysis: Infrared intensities has been computed analytically using DFT wave functions with M06/6-311G and are listed in Table-2, including experimental values[4]. As the appropriate scaling factors for M06 DFT was not seen, that of M06-2X/6-31(2df,p) was used[14]. On the contrary, experimental data in Figure-4 did not show frequencies between 2800 and 1700 cm^{-1} which correspond to the hybridized carbon of

aromatic cycles. On the other hand, it detects the non-chelated hydroxyl group at 3497 cm^{-1} that is undetected in experimental data. The strong peak at 3396 cm^{-1} indicates the chelated hydroxyl of the title compound, while the medium peak at 3202 and 1200 cm^{-1} correspond to the ether group. The wave numbers at 2953-2851 cm^{-1} identify the methyl and methylene group of smeatxanthone A. The peak at 1601 cm^{-1} is for O-hydroxy-aryl ketone, whereas those at 1447 and 1290 cm^{-1} clearly reveal respectively alkene and methyl of the geranyl group. Finally, the last weak peaks are attributed to for alkene functions of the geranyl substituent.

Table-2: Computed and experimental IR data of smeathxanthone A

Experimental IR[4]	Unscaled frequencies	Scaled frequencies
	3673	3497
3315	3566	3396
2891	3432, 3363	3202,2851
2351	-	-
2200	-	-
1961	-	-
1579	1681	1601
1440	1520	1447
1290	1349	1295
1193	1239	1180
1084	1152	1092
936	1015	967
822	864	823
784	803	789

Fukui functions: The Fukui function can be calculated in Jaguar program[10]. These functions can be very important to locate chemical reactivity indices of a molecule[15]. In this work, the values of Fukui functions have been mapped to the electron density and obtained using the isovalue 0.001. Figure-5 and Figure-6 show the f$^+$ and f$^-$ respectively. Blue or purple color illustrates areas where function possesses positive values, while red or orange color illustrates the areas where function is having negative values. The f$^-$ and f$^+$ are pretty much the same for the title compound and show that positive values for f$^+$ are located in the hydrogen atoms and can act as electrophile while the negative values for f$^-$ are located in the oxygen atom which can act as nucleophile.
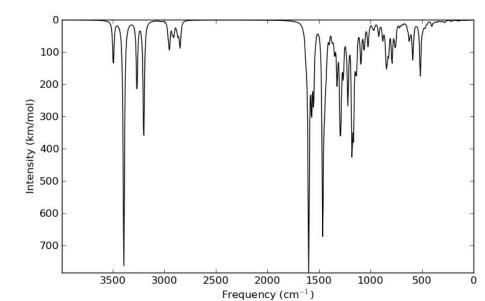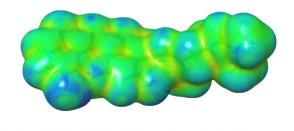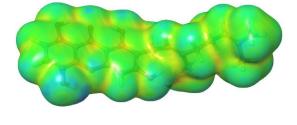
Figure-4: Scaled IR spectra of smeathxanthone A.

Figure-5: Fukui function f⁺ of smeathxanthone A.

Figure-6: Fukui function f⁻ of smeathxanthone A.

Figure-7: MEP plot of smeathxanthone A.

Molecular electrostatic potential: Electrostatic potential surfaces mapped with electron density is now in the list of well-establish methods able toreveal the reactivity of organic functional groups through their electronic properties[16, 17]. Visually this can be plotted with electron density surfaces using rainbow colors in the increasing order of their wavelength. Such maps are able to clearly illustrate electronic variations in a molecule and consequently give electrophilic and nucleophilic areas[18]. On Figure-7, the negative charges colored in red in the electronic map correspond to electrophilic sites and the most negative are occupied here by the hydrogen and carbon atoms. The positive region, colored in blue over the electronic map correspond to nucleophilic sites and the most positive are occupied by the carbonyl and hydroxyl groups.
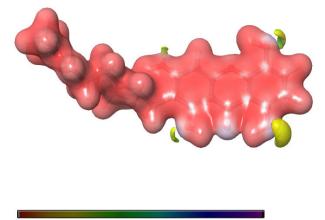
Frontier molecular orbital analysis: Molecular orbitals computation is of great importance for quantum chemistry[19], and therefore has been usually used to explain transition states reactivity in chemical reactions. In the present work B3LYP/6-311G has been used for computation. Calculated orbitals (HOMO, LUMO) could be associated with reactivity and pharmaceutical properties of a compound[20]. Compounds with small orbital energy gap generally present highly reactive moieties and global instability[21]. Figure-8 shows the HOMO and LUMO. In smeathxanthone A the highest occupied orbitals of π nature override the C ring and pyran-4-one cycle whereas the lowest unoccupied orbitals override the carbonyl groups and carbon atoms. From their energies which are -0.0099217096 eV and -0.0040718904 eV respectively we calculate the gap ΔE = 0.0058 eV. This low energy gap is due to the solvent and shows that the molecule is highly reactive. In Figure-9, the LUMO+1 are very similar to the LUMO orbitals whereas the HOMO-1 orbitals are located in the geranylsubstituent. The energy gap between these last orbitals is 0.1648 eV.
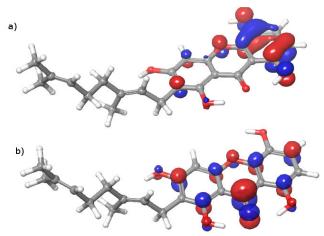
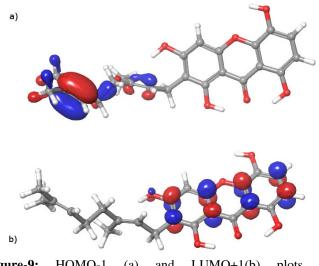**Figure-8:** HOMO (a) and LUMO (b) plots ofsmeathxanthone A.

Figure-9: HOMO-1 (a) and LUMO+1(b) plots of smeathxanthone A.

Conclusion

The structure of smeathxanthone A was studied in the liquid phase by the M06/6-311G method. The optimized geometry was in very good conformity with the crystal structure except for the 3-hydroxyl group which is oriented towards the geranylsubstituent. A vibrational analysis was performed and an IR spectra in good terms with data obtained from experiments has been plotted. Molecular electrostatic potential, LUMO and HOMO were performed to reveal the electronic characteristics of the molecule. MEP has the highest negative points at the level of the hydroxyl and carboxyl groups. Fukui functions mapped with electronic density confirmed the nucleophilic potential of oxygen in the title compound. Difference of energy between the highest occupied and lowest unoccupied orbitals allows us to demonstrate the high reactivity of the title compound. All this allowed us to demonstrate the stability of the molecule in aqueous medium, which offers a certain therapeutic potential.

References

1. Peres V., Nagem T.J., and de Oliveira F.F. (2000). Tetraoxygenated naturally occurring xanthones. Phytochemistry, 55(7), 683-710.

2. Masters K.S., and Bräse S. (2012). Xanthones from fungi, lichens, and bacteria: the natural products and their synthesis. Chemical reviews, 112(7), 3717-3776.

3. Marston A., Hamburger M., Sordat-Diserens I., Msonthi J. D., and Hostettmann K. (1993). Xanthones from Polygala nyikensis. _Phytochemistry_, 33(4), 809-812.

4. Komguem J., Meli A.L., Manfouo R.N., Lontsi D., Ngounou F.N., Kuete V. and Connolly J.D. (2005). Xanthones from Garciniasmeathmannii (Oliver) and their antimicrobial activity. _Phytochemistry_, 66, 1713-1717.

5. Roberts J.C. (1961). Naturally Occurring Xanthones. _Chemical Reviews_, 61(6), 591-605.

6. Nakanishi W., Hayashi S., Kusuyama Y., Negoro T., Masuda S. and Mutoh H. (1998). Why Selenoxanthone Gives an MC with Bromine: An Examination of Electronic States of Xanthones and Xanthenes by Electron Spectroscopy and ab Initio MO Calculations. _The Journal of Organic Chemistry_, 63(23), 8373-8379.

7. Sugino T., Kambe N., Sonoda N., Sakaguchi T., and Ohta K. (1996). Ab initio molecular orbital calculations of the static polarizabilities of xanthone analogues. _Chemical physicsletters_, 251(3-4), 125-131.

8. Gonçalves N.S., Cristiano R., Pizzolatti M.G. and da Silva Miranda F. (2005). Vibrational analysis and NMR properties based on ab initio and DFT calculations of two naturally occurring xanthones: 1, 5-dihydroxy-2, 3-dimethoxyxanthone and 1-hydroxy-5-methoxy-2, 3-methylenedioxyxanthone. _Journal of molecular structure_, 733(1), 53-61.

9. Zhao Y. and Truhlar D.G. (2008). The M06 suite of density functionals for main group thermochemistry, thermochemical kinetics, noncovalent interactions, excited states, and transition elements: Two new functionals and systematic testing of four M06-class functionals and 12 other functionals. _Theor. Chem. Account._, 120, 215-241.

10. Bochevarov A.D., Harder E., Hughes T.F., Greenwood J. R., Braden D.A., Philipp D.M., Rinaldo D., Halls M.D., Zhang J. and Friesner R.A. (2013). Jaguar: A High-Performance Quantum Chemistry Software Program with Strengths in Life and Materials Sciences. _Int. J. Quantum Chem._, 113(18), 2110-2142.

11. Becke A.D. (1993). Density-functional thermochemistry. III. The role of exact exchange. *The Journal of chemicalphysics*, 98(7), 5648-5652.

12. Lee C., Yang W. and Parr R.G. (1988). Development of the Colle-Salvetti correlation-energy formula into a functional of the electron density. *Physical review B*, 37(2), 785-789.

13. Choudhary M.I., Swaleh R., Anjum S., Lannang A.M., Ali S. and Fun H.K. (2005). 2-(3, 7-Dimethylocta-2, 6-dienyl)-1, 3, 5, 8-tetrahydroxyxanthone. *Acta Crystallographica Section E*: Structure Reports Online, 61(12), o4313-o4315.

14. National Institute of Standards and Technology. http://cccbdb.nist.gov/vibscalejust.asp.23/04/2017

15. Ghosh D., Hazra S., Pal P. and Misra T.N. (1993). Spectroscopic, dark and photoconductive properties of some polyene-iodine charge-transfer complexes. *Bulletin of Materials Science*, 16(2), 127-135.

16. Politzer P. and Murray J.S. (1991). Molecular electrostatic potentials and chemical reactivity. *Reviews in Computational Chemistry*, 2, 273-312.

17. Goss D.J. and Petrucci R.H. (2007). General Chemistry Principles and Modern Applications, Petrucci, Harwood, Herring, Madura: Study Guide. Pearson/Prentice Hall.

18. Politzer P. and Murray J.S. (2002). The fundamental nature and role of the electrostatic potential in atoms and molecules. Theoretical Chemistry Accounts: Theory, Computation, and Modeling (Theoretica Chimica Acta), 108(3), 134-142.

19. Gunasekaran S., Kumaresan S., Balaji R.A., Anand G. and Seshadri S. (2008). Vibrational spectra and normal coordinate analysis on structure of chlorambucil and thioguanine. *Pramana: Journal of Physics*, 71(6).

20. Sajan D., Lakshmi K.U., Erdogdu Y. and Joe I.H. (2011). Molecular structure and vibrational spectra of 2, 6-bis (benzylidene) cyclohexanone: a density functional theoretical study. *Spectrochimica Acta Part A: Molecular and Biomolecular Spectroscopy*, 78(1), 113-121.

21. Sinha L., Prasad O., Narayan V. and Shukla S.R. (2011). Raman, FT-IR spectroscopic analysis and first-order hyperpolarisability of 3-benzoyl-5-chlorouracil by first principles. *Molecular Simulation*, 37(2), 153-163.